Med. & Biol. Eng. & Comput., 1982, 20, 299–306

Linear and nonlinear properties of platinum electrode polarisation. Part 1: frequency dependence at very low frequencies

B. Onaral* **H. P. Schwan**

Department of Bioengineering, University of Pennsylvania, Philadelphia, PA 19104, USA

*Electrical and Computer Engineering Department, Drexel University, Philadelphia, PA 19104, USA

Abstract—*The polarisation impedance of the platinum electrode was measured in physiological saline (0·9% NaCl) over six decades of frequencies down to 1 mHz. The applicability of Fricke's phase angle rule was verified down to 10 mHz. The resistive shunt which emerges at lower frequencies was shown to be equivalent to the direct current (d.c.) impedance of the interface. A Cole–Cole (1941) type of relaxation model is proposed to describe the interface behaviour over all frequency ranges. Nonlinear polarisation measurements have demonstrated the validity of Schwan's limit law of linearity at very low frequencies.*

Keywords—*Electrode polarisation, Platinum electrodes*

1 Introduction

THIS research aims at a phenomenological study of the very low-frequency behaviour of the platinum electrode interface in the absence of an imposed or induced d.c. potential and in an environment simulating physiological conditions. The Pt electrode is widely used in physiological measurements and stimulation applications, yet there is a lack of knowledge of its properties at very low frequencies.

The polarisation impedance of the platinum electrode has been investigated over an extended frequency range, and many models have been suggested to describe the observed frequency dependence. Warburg's classical model (WARBURG, 1899, 1901) characterises the polarisation impedance Z_p as a series combination of the resistance R_p with a capacitance C_p, and states that both change proportionally with the square root of the frequency f. The phase angle

$$\delta = \tan^{-1}(R_p \omega C_p) \quad . \quad . \quad . \quad . \quad . \quad . \quad . \quad (1)$$

is frequency independent and has a value of 45°. Here ω is the angular frequency. FRICKE (1932) recognised that the polarisation capacitance and resistance are better described as power functions of the frequency:

$$C_p \sim f^{-m}$$

$$R_p \sim f^{m-1} \quad . \quad . \quad . \quad . \quad . \quad . \quad . \quad . \quad . \quad . \quad (2)$$

and formulated the relationship between the phase angle δ and the power factor m:

$$\delta = m\pi/2 \quad . \quad . \quad . \quad . \quad . \quad . \quad . \quad . \quad . \quad . \quad (3)$$

Fricke's rule above follows from Kramers–Kronig formulae (DANIEL, 1967) for a power function representation of the polarisation capacitance as in eqn. 2, only if m is independent of frequency.

SCHWAN (1963, 1966) explored the frequency range from 20 Hz to 200 kHz and noted that the power factor m in Fricke's formulation for the polarisation capacitance changes with frequency from a value of about 0·3 to 0·5 as the frequency increases from 20 Hz to 200 kHz; nevertheless, these data agree well with Fricke's rule (eqn. 3), which assumes a frequency independent power factor. In an attempt to account for the variations of m with frequency, JARON *et al.* (1968) modelled the electrode interface as a series combination of a frequency independent 'blocking' capacitor with a Warburg element characterised by a 45° phase angle. But DE BOER and VAN OOSTEROM (1978) have returned to Fricke's model in their investigation of the electrical properties of platinum electrodes.

Most models for the metal electrode-electrolyte

*Present address of B. Onaral: Electrical and Computer Engineering Department, Drexel University, Philadelphia, PA 19104, USA

First received 19th December 1980 and in final form 21st July 1981

0140–0118/82/030299+08 $01·50/0

interface are motivated by the desire to fit experimental data and be consistent with electrochemical considerations. For example, Warburg's (1899, 1901) initial theory on electrode polarisation was based on a diffusion model. Fricke's (1932) frequency dependance law, on the other hand, was suggested by a survey of existing polarisation impedance measurements over a limited frequency range. Similarly, JARON *et al.* (1968) set out to better fit experimental data with their model. GRAHAME (1946, 1952) after demonstrating the absence of frequency dispersion in the case of a dropping mercury electrode, claimed that the surface state of solid electrodes is responsible for the frequency dependent properties of the interface. An entirely new concept was introduced by SCHEIDER (1977), who demonstrated that the lateral charge transfer along the irregular surface is the major cause of the fractional power frequency dependence, thereby emphasising the importance of surface roughness. BOCKRIS *et al.* (1966) suggested that differently structured water near the electrode surface may be responsible for observed frequency dependencies.

Electrochemical considerations have been translated into various models. SLUYTERS-REHBACH and SLUYTERS (1970) have compiled a comprehensive review of popular equivalent circuits with and without the coupling mechanism. The classical RANDLES (1947) model is of the first kind. The model developed by TIMMER *et al.* (1968) is a typical example of the second. Usually very complex models result.

Most of these models predict an infinite polarisation impedance as the frequency approaches zero, for they do not provide a path for the passage of direct currents. And yet, the polarisation impedance of metal electrodes assumes a finite value at very low frequencies, often below 10 mHz, equal to the interface resistance R_{DC} determined from the slope of the d.c. voltage-current characteristic (GABRIELLI and KEDDAM, 1974). This suggests that C_p in the series model must eventually change with $f^{-m}(m \geqslant 1)$ at very low frequencies, and that R_p must reach a constant value. Hence, a question arises as to the validity of Fricke's phase angle law in this range of frequencies.

SIMPSON *et al.* (1980) have extended the range of linear measurements down to 0·1 Hz. They observed Fricke's rule to be obeyed at these frequencies. They also conducted a limited number of measurements at lower frequencies and realised the need for a shunting resistance R_{DC} across the polarisation impedance.

All of the above cited work is concerned with linear aspects of electrode polarisation, i.e. polarisation impedances independent of signal strength. Limits of this linear behaviour were investigated by SCHWAN and MACZUK (1965) and GEDDES *et al.* (1971) and a non-linearity rule was formulated by SCHWAN (1968) as follows:

$$i_L \sim f^{1-m} \quad . \quad . \quad . \quad . \quad . \quad . \quad . \quad . \quad . \quad . \quad (4)$$

Here i_L the limit current of linearity is that current where C_p and R_p deviate by 10% from the values observed at low current densities. m is the above defined Fricke power factor (eqn. 2), but need not be constant with respect to the frequency. This relationship has been experimentally confirmed at frequencies as low as 1 Hz (SIMPSON, 1976). However, its validity would be questioned at lower frequencies where one must expect strong deviations from the predictions of models neglecting the d.c. shunt resistance.

2 Methods

The polarisation impedance data presented in this paper cover six decades of frequency down to 1 mHz. Measurements were conducted with a frequency response analyser (EMI-SE Labs: SM 2001)*. GREEF (1978) refers to the frequency response analyser technique based on input-output signal correlation as a most advanced automated electrode interface impedance measurements tool. This technique was applied to electrode studies initially by Epelboin's groups (EPELBOIN *et al.*, 1970; EPELBOIN *et al.*, 1973; GABRIELLI and KEDDAM, 1974; GABRIELLI *et al.*, 1977) and somewhat later by ARMSTRONG *et al.* (1977). On-line measurements of bioelectrode impedances down to a frequency range of 5 mHz have been achieved in Schmitt's laboratory (ALMASI *et al.*, 1968; ALMASI and SCHMITT, 1974). Several other laboratories have devised similar techniques (MOHILNER *et al.*, 1976; BURBANK and WEBSTER, 1978).

Other investigators have used analogue techniques to measure electrode impedances at low frequencies (MURDOCK and ZIMMERMAN, 1936; SIMPSON, 1976; DE BOER and VAN OOSTEROM, 1978). We chose the digital technique since it offers drastic reduction in measurement time at very low frequencies. Also, digital equipment can be readily programmed. Other beneficial features are freedom from noise, distortion and drift in signal generation and detection.

In its basic mode, LFRA allows the computation of the transfer characteristics of the test system. However, it can be modified to conduct impedance measurements. This isaccomplished by measurement of the monitored voltages and currents across the load using a voltage division scheme. The generator output voltage is impressed upon the electrode cell in series with a known reference resistance connected to earth. The correlator detects the voltage drop across the reference resistance. The value of the unknown impedance phasor is calculated using appropriate circuit equations. An optimum choice of the reference resistance is dictated by resolution considerations. We achieved an amplitude resolution of better than 0·01 dB (0·12%) over most of the measurement range covered in the present article. A comparable resolution in the phase angle ϕ was assured as long as the latter

** Courtesy of EMI-SE Labs. Ltd., Middlesex, England: Scientific Devices Co., New Jersey, USA*

lay between approximately 15° to 75°. At extremely low frequencies, where the quadrature component of the impedance is reduced to a fraction of the in-phase component, the resolution in-phase was somewhat reduced.

The electrode impedance measurements described here were performed by controlling the input voltage signal applied to the electrode interface.

Electrode research aimed at deciphering the electrochemical processes at the electrode-electrolyte interface requires rigorous control of all the factors involved. However, if electrode polarisation investigations do serve the purpose of phenomenological description within a physiological environment, the use of high purity techniques becomes unnecessary. The human body is far removed from a well controlled system as far as electrode electrochemistry is concerned and extrapolation of results obtained in such systems to *in vivo* conditions should be made with the greatest care (SILVERMAN *et al.*, 1973).

The electrodes used in the study were made of platinum wires sealed in Pyrex glass tubing. The exposed surface is flat and polished prior to etching in boiling aqua regia. Observation under the microscope revealed a randomly varying microscopic surface state. It was expected that adhering to the same polishing and etching routines would result in macroscopically similar working surfaces. Freshly prepared electrodes were stabilised according to aging techniques suggested by SCHWAN (1966). The macroscopic surface area was 0·855 cm^2.

The test electrodes were measured against a large area platinum counter-electrode platinised according to the conventional Kohlrausch procedure (1897), using current densities suggested previously by SCHWAN (1963, 1966). Three-point measurements may also be carried out with the same cell. The latter mode is used in transient measurements, and the third platinum electrode is a sensing (reference) electrode in the form of a circular loop.

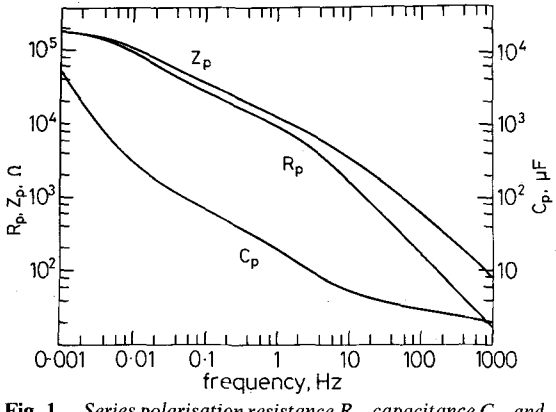

Fig. 1 *Series polarisation resistance R_p, capacitance C_p, and impedance Z_p against frequency. Pt electrode; geometrical ares: 0·0855 cm^2; linear measurement (65 mV); 0·9% NaCl; pH: 6·5 ± 0·1; T : 25 ± 1°C*

The measurements were conducted in physiological saline (0·9% NaCl). A group of measurements were repeated in human blood serum and results were quite similar. The electrolyte temperature was controlled at 25° ± 1°, and the pH monitored throughout the experiments for reproducibility of results.

The data in this study have been corrected for the effect of the electrolyte resistance R_{el} using a method suggested before (SCHWAN, 1963). The overpotential in response to an alternating current or voltage signal is superimposed on the equilibrium cell (d.c.) potential which is equal to the algebraic sum of the half-cell potentials of the test and the counter electrode. The small a.c. signal properties of the interface at various d.c. potentials have been investigated (SIMPSON *et al.*, 1980). In the absence of induced or imposed d.c. bias, a residual potential exists even if the two electrodes are made of the same metal. In this study, the large counter electrode was platinised; therefore, a residual potential was unavoidable due to surface discrepancies. To conduct measurements at the identical equilibrium potential, the measurement procedure outlined in the next paragraph was closely followed.

The polarisation impedance exhibits hysteresis if nonlinear measurements are conducted first with increasing and then decreasing signal strengths. The discrepancy becomes increasingly noticeable when signal levels are well in excess of the limit of linearity (more than 10% deviation from linearity). These effects can be attributed to a.c. induced rectification which apparently raises the interface equilibrium potential from its original resting level (KAHN and GREATBATCH, 1974; DYMOND, 1976). We used a method to indirectly verify and remedy for hysteresis. This method is based on the depolarising effect of alternating current (a.c.) signals on the interface (SIMPSON *et al.*, 1980; VENKATESH and CHIN, 1979). It consisted of repeating after each measurement an initial measurement made at the same frequency but with a much smaller signal amplitude (approximately 30 mV). We continuously pulsed the interface with this a.c. signal until the same result was reproduced. We observed that the waiting period increased as the electrode was driven further into nonlinearity. Indeed, no waiting period was necessary for measurements in the linear range. The method was modified for frequencies below 1 Hz, such that the return to a fixed measurement point (e.g., 100 Hz, 30 mV) was considered a satisfactory verification of interface recovery. If recovery was not possible in a reasonable period of time, the experiment was ended and the electrode surface was retreated.

3 Results

Linear platinum electrode polarisation results are presented in Figs. 1 and 2. The linearity was ascertained at each measurement point by the independence of measured values from the input signal strength. The frequency dependence of the polarisation impedance Z_p, the series polarisation

resistance R_p, and the capacitance C_p are shown in Fig. 1. Below 10 mHz, C_p is observed to increase sharply, whereas R_p tends towards a constant value. Fig. 2

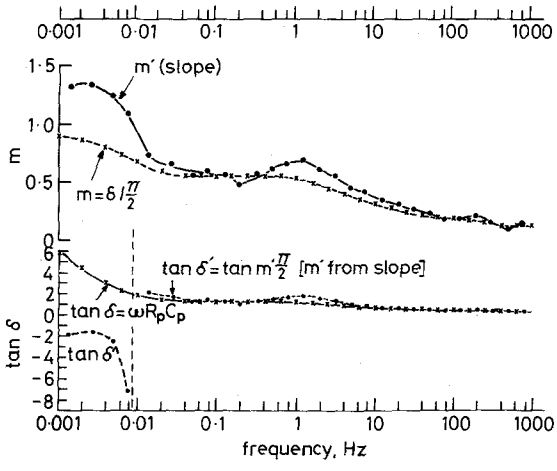

Fig. 2 *The frequency dependence of the parameter m deducted from the loss tangent tan δ using Fricke's rule (eqn. 3) and the power factor m' determined from the slope of the measured C_p against frequency curve in the log-log presentation. The measured loss tangent tan δ and the loss tangent tan δ' calculated from m' using Fricke's rule. Electrode system as in Fig. 1*

compares the value of the power factor m' determined from the slope of C_p against frequency curve to the factor m deduced from the measured loss angle δ using Fricke's law (eqn. 3). Both the m and m' values agree in the range of frequencies from 10 mHz to 400 mHz and above 10 Hz. The respective loss tangents are also included in the figure. The data of Fig. 1 are displayed in Fig. 3 in the form of an impedance locus plot with frequency as a parameter. Extrapolation of this locus would suggest a d.c. impedance of about 200 kΩ. As a verification of this extrapolation, we conducted d.c. measurements. The interface resistance was found to deviate less than 15% from the R_p value at 1 mHz.

The study of interface non-linearity is extended to various frequencies in Figs. 4, 5 and 6. Fig. 4 shows the polarisation voltage-current characteristic at three different frequencies plotted in the form of Tafel curves. Essentially identical curves result except for a shift to

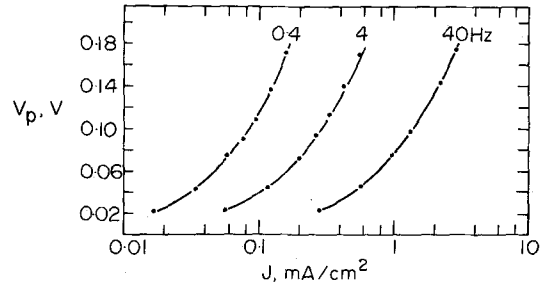

Fig. 4 *Semilogarithmic voltage-current characteristics at 0·4, 4 and 40 Hz. Electrode system as in Fig. 1*

higher current densities as the frequency is increased. Figs. 5 and 6 display various interface properties as a function of the overpotential in a frequency range from 100 Hz down to 4 mHz. The onset of nonlinearity appears virtually independent of frequency and occurs near an overpotential of 100 mV (Fig. 5). A more detailed analysis is presented in Fig. 6. Several percentage figures are calculated from 4 and 20 mHz curves at an overpotential of 120 mV and are quite comparable. The interface impedance Z_p and the polarisation capacitance C_p exhibit a 10% deviation from linearity at approximately 131 mV, whereas the resistance R_p deviates by 13·5%, indicating a small change of 2·8% in tan δ.

Fig. 7 compares the frequency dependence of the limit current of linearity determined from the 10% deviation of the polarisation impedance from its linear

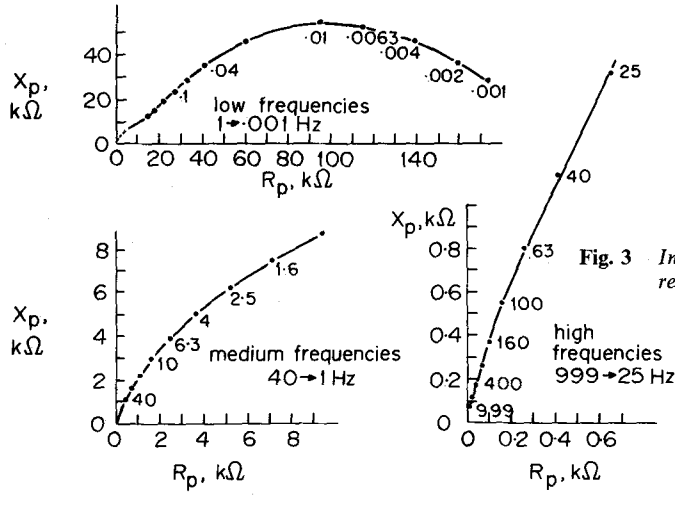

Fig. 3 *Impedance plane locus plot of the polarisation resistance and reactance. Electrode system as in Fig. 1*

value (top curve) to the behaviour of the polarisation current when the overpotential is maintained at 100 mV (middle curve) and 65 mV (bottom curve). The

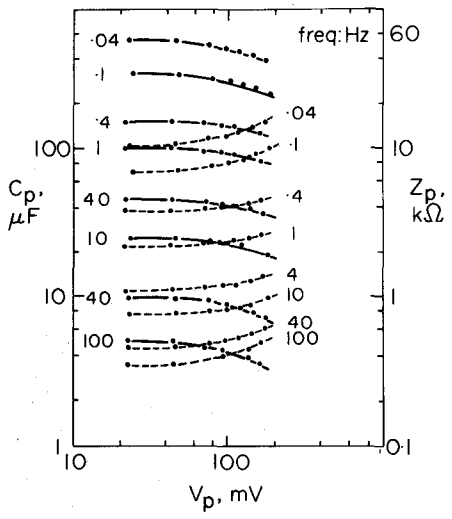

Fig. 5 *Interface impedance and series capacitance as a function of the overpotential with frequency as parameter. Electrode system as in Fig. 1. Solid lines: Z_p; Dashed lines: C_p*

numbers on the top curve pertain to overpotential levels. An average of 117·3 mV was established from these values (standard deviation: 7·64 mV; standard error of the mean: 2·7 mV). Fig. 8 displays similar results extracted from a different set of measurements. Here the limit current of linearity is plotted together with the interface current at the average limit voltage of linearity ($\bar{V}_p$ = 128 mV for this particular set). The interface admittance Y_p, measured at an overpotential of 65 mV, is also included in the same figure for comparison. A rather small systematic variation of the quoted V_p values along the upper curve of Fig. 7 is

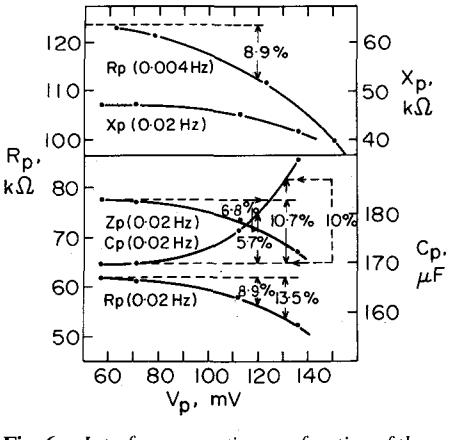

Fig. 6 *Interface properties as a function of the overpotential at 4 and 20 mHz. Electrode system as in Fig. 1*

noticeable, suggesting that the frequency dependence of the limit current of linearity corresponds to a boundary potential which is almost constant as the frequency is varied over six decades. This systematic variation of V_p could not be reproduced, as is apparent from Fig. 8. Here, the polarisation potential of 128 mV corresponds almost perfectly to the onset of nonlinearity at the 10% level over the entire frequency range.

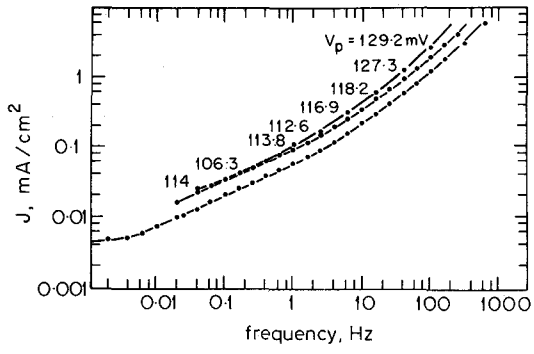

Fig. 7 *Top curve: the frequency dependence of the limit current of linearity determined at 10% deviation of Z_p from its linear value. Middle curve: the interface current density at an overpotential of 100 mV. Bottom curve: the interface current at an overpotential of 65 mV. The solid circles on this curve are taken from two different sets of experiments. The electrode system as in Fig. 1*

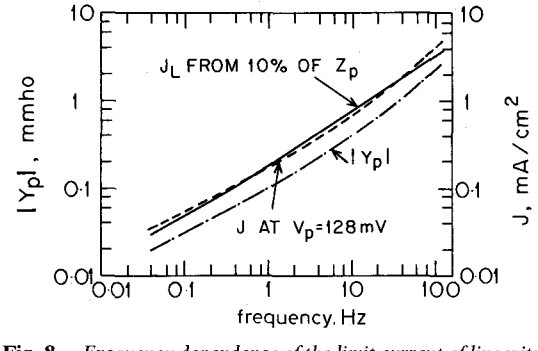

Fig. 8 *Frequency dependence of the limit current of linearity at 10% deviation of Z_p from its linear value and the interface current density at the average limit voltage of linearity (128 mV). The magnitude of the linear interface admittance versus frequency is also included for comparison. The electrode system as in Fig. 1*

4 Discussion

The data presented in Fig. 1 appear to support the approximate validity of Fricke's phase angle rule (eqn. 3) down to 10 mHz. There is, however, some discrepancy between the predictions of this rule and the data presented in Fig. 2. Here the power factor m', determined from the slope of the C_p against frequency

curve in Fig. 1, and the parameter m, calculated from the loss angle δ using Fricke's rule, correlate well only over the limited ranges of frequency from about 10 mHz to 400 mHz and above 10 Hz. It is not coincidence that in the same frequency ranges, the value of m' remains fairly constant. Kramers–Kronig relationships demand that for an extended range of frequencies in which the power factor m' remains constant, Fricke's rule be followed. However, towards both ends of the range, the data can be expected to deviate from the prediction of this rule, depending on the error introduced by integrating the extrapolated frequency behaviour outside the range of validity. This probably causes the discrepancy between the values of m and m' and the respective tangents, $\tan\delta$ and $\tan\delta'$ (Fig. 2), in the interval from 400 mHz up to 10 Hz. The inapplicability of Fricke's rule below 10 mHz, however, calls for an entirely different interpretation of the interface properties.

The impedance locus presented in Fig. 3 can be approximated by a circle with a suppressed centre. This circle may be presented by the impedance function.

$$Z_p = \frac{Z_{DC}}{1+(j\omega\tau_0)^{\beta}} + b \quad . \quad . \quad . \quad . \quad . \quad . \quad (5)$$

with $b = 0$ since the circle connects with the origin of the impedance plane and Z_{DC} the zero frequency impedance given by the other intercept of the circle with the resistance axis. In this expression τ_0 is an average time constant, assuming a Cole-Cole distribution function of time constants (Cole and Cole, 1941) and $\beta = 1-m$, where m is the power factor in eqn. 2. The inverse of Z_p, the admittance,

$$Y_p = \frac{1}{Z_{DC}} + \frac{(j\omega\tau_0)^{\beta}}{Z_{DC}} \quad . \quad . \quad . \quad . \quad . \quad . \quad (6)$$

is a parallel combination of a shunt resistance Z_{DC} and a constant phase angle impedance element of the form $(j\omega\tau_0)^{-\beta}$ as proposed by Fricke. For high frequencies

$$Z_p = Z_{DC}(\omega\tau_0)^{-\beta}e^{-j\beta\pi/2} \quad . \quad . \quad . \quad . \quad . \quad . \quad (7)$$

and X/R is given simply by $\tan\left(-\beta\frac{\pi}{2}\right)$. Since the circle centre is located below the real axis, β must be positive and smaller than one, which is consistent with the model.

This model can be only approximate, but it serves well enough to summarise several essential features:

(i) The emergence of a resistive shunt given by the d.c. impedance. At frequencies below 10 mHz the polarisation impedance, as extrapolated from higher frequencies, becomes larger than this shunt and, hence, this shunt increasingly dominates.

(ii) The existence of an average time constant which is characterised by the average relaxation frequency $f_0 = 1/2\pi\tau_0$ where the circle peaks. For $f_0 = 10$ mHz, the time constant is $\tau_0 = 16{\cdot}2$ s.

For frequencies above the relaxation frequency f_0 the electrode behaviour is best presented by whatever is the appropriate polarisation model; and for frequencies below, by the d.c. resistance. Tan δ does not change strongly for frequencies above f_0. But below this value, tan δ increases more rapidly and must approach infinity as the d.c. shunt increasingly dominates. The results presented in Figs. 1, 2 and 3 are largely consistent with this description.

The electrode-electrolyte interface behaves non-linearly if the excitation current exceeds a critical value, the 'limit current of linearity', at a given frequency. The limit law of linearity (eqn. 4) was formulated to relate the frequency dependence of the limit current values to the frequency dependence of the series polarisation capacitance ($C_p \sim f^{-m}$). An identical solution is obtained if the frequency dependence of C_p is substituted by that of the polarisation admittance magnitude ($|Y| \sim f^{1-m}$). This transformation is justified by the observation that $\tan\delta$ changes only a little with increased current density. Thus the onset of nonlinearity can be predicted from the frequency dependence of the linear polarisation admittance (or impedance).

The limit of linearity experiments performed before in this laboratory initially covered frequencies between 20 Hz to 200 kHz (SCHWAN, 1966) and then frequencies down to 0·1 Hz (SIMPSON *et al.*, 1980). We conducted limit of linearity measurements in a frequency range from a few mHz up to 1 kHz.

In Fig. 4, the semilogarithmic dependence of the interface potential on current right at the exit from linearity is precisely the behaviour described by the empirical Tafel relationship formulated for the d.c. case. The results in this figure experimentally verify the generalisation of Tafel's law to the a.c. case. The interface impedance magnitude and the series capacitance are plotted against the overpotential in Fig. 5 with the frequency varying from 40 mHz to 100 Hz as a parameter. The onset of nonlinearity at 20 mHz and 4 mHz is studied in Fig. 6. The weaker dependence of the tan δ profile on the strength of the input stimulus at the emergence of nonlinearity is verified at 20 mHz by the close match between the 10% deviation point on the polarisation resistance and capacitance curves. Another important observation from these results is that the value of the overpotential at the emergence of nolinearity is frequency independent over the investigated range of frequencies.

It is well established that the electrode-electrolyte interface lends itself to small signal analysis. This implies that at a given static bias (linear or nonlinear) one can measure the properties of the interface in a linear fashion (GABRIELLI and KEDDAM, 1974; MCDONALD, 1971). Therefore, laws such as the 'limit of linearity' must hold in the presence of imposed or

induced (a.c. rectification) d.c. bias. SIMPSON *et al.* (1980) have investigated the effect of imposed d.c. bias on the limit law of linearity and detected only a subtle dependence. Our results have similarly demonstrated that induced d.c. bias does not significantly affect the behaviour of the interface at the onset of nonlinearity in terms of the overpotential.

This study concludes with an experimental verification of the frequency dependence of the limit current of linearity as predicted by eqn. 4. Results from two independent sets of measurements are summarised in Figs. 7 and 8. The current densities determined at the point where the polarisation impedance deviates by 10% from its linear value form a frequency dependent 'limit of linearity curve'. In Fig. 7, one such curve is compared to the polarisation current characteristics when the overpotential is maintained at 65 mV and 100 mV. Indeed, Ohm's law demands that, for a constant voltage applied to a linear admittance, the response current assume the frequency dependence of this admittance. The limit of linearity curve in Fig. 8 is directly compared to the interface admittance measured at an overpotential of 65 mV. The third curve in this last figure displays the frequency dependence of the interface current at the average limit voltage of linearity for this particular set, thereby confirming the frequency independence of the overpotential level at which nonlinearity emerges.

The data of Figs. 7 and 8 demonstrate that the limit current of linearity changes approximately with the square root of frequency. Departures from this behaviour reflect similar polarisation admittance deviations from a Warburg or Fricke model. Only in one case were data obtained below 0·01 Hz. Fig. 7 presents current densities yielding a frequency independent boundary potential of 65 mV. These data are almost frequency independent below 10 mHz, predicting that the d.c. impedance approaches nonlinearity at a boundary potential of 65 mV corresponding to a current density of about 4 μA/cm^2. This would correspond with a nonlinearity at the 10% level occurring at a potential of 120 mV and a current density of about 7 μA/cm^2.

References

ALMASI, J. J., HART, M. W. and SCMITT, O. H. (1968) On-line measurement of biological impedance at very low frequencies. *Biophys. J.*, **8**, A45.

ALMASI, J. J. and SCHMITT, O. H. (1974) Automated measurement of bioelectric impedance at very low frequencies. *Comp. Biomed. Res.*, **7**, 449.

ARMSTRONG, R. D., BELL, M. F. and METCALFE, A. A. (1977) A method for automatic impedance measurement and analysis. *J. Electroanal. Chem.*, **77**, 287.

BOCKRIS, J. O'M., GILEADI, E. and MÜLLER, K. (1966) Dielectric relaxation in the electric double layer. *J. Chem. Phys.*, **44**, 1, 1445.

BOER, R. W. DE and VAN OOSTEROM, A. (1978) Electrical properties of platinum electrodes: impedance measurements and time domain analysis. *Med. & Biol. Eng. & Comput.*, **16**, 1–10.

BURBANK, D. P. and WEBSTER, J. G. (1978) Reducing skin potential motion artefact by skin abrasion. *Med. & Biol. Eng. & Comput.* **16**, 31–38.

COLE, K. S. and COLE, R. H. (1941) Dispersion and absorption in dielectrics. I. Alternating current characteristics. *J. Chem. Phys.*, **9**, 341.

DANIEL, V. V. (1967) *Dielectric relaxation.* Academic Press, New York, London.

DYMOND, A. (1976) Characteristics of the metal-tissue interface of stimulation electrodes. *IEEE Trans.*, **BME-23**, 4, 274.

EPELBOIN, I., GABRIELLI, C. and LESTRADE, J. C. (1970) Étude et réalization d'un potentiostat destiné aux mesures d'impédance électrochimique entre 10^{-5} et 50 kHz. *Revue Générale de l'Electricité*, **79**, 669.

EPELBOIN, I., KEDDAM, M. and LESTRADE, J. C. (1973) Faradaic impedances and intermediates in electrochemical reactions. *Faraday Discuss. Chem. Soc.*, **56**, 264.

FRICKE, H. (1932) The theory of electrolytic polarisation, *Philo. Mag.*, **14**, 310.

GABRIELLI, C. and KEDDAM, M. (1974) Progrès récent dans la mesure des impédances electrochimiques en régime sinusoidal. *Electrochimica Acta*, **19**, 355.

GABRIELLI, C., KSOURI, M. and WIART, R. (1977) Compensation de la chute ohmique par une méthode analogique. Application a la mesure des impédances electrochimiques et à la détermination des courbes de polarization. *Electrochimica Acta*, **22**, 255.

GEDDES, L. A., DA COSTA, C. P. and WISE G. (1971) The impedance of stainless-steel electrodes. *Med. & Biol. Eng.*, **9**, 511.

GRAHAME, D. C. (1946) Properties of the electrical double layer at a mercury surface. II. The effect of frequency on the capacity and resistance of ideally polarized electrodes. *J. Am. Chem. Soc.*, **68**, 301.

GRAHAME, D. C. (1952) Mathematical theory of faradaic admittance. *J. Electrochem. Soc.*, **99**, 370c.

GREEF, R. (1978) Instruments for use in electrode process research. *J. Phys. E.: Sci. Instrum.*, **11**, 1.

JARON, D., SCHWAN, H. P. and GESELOWITZ, D. B. (1968) A mathematical model for the polarization impedance of cardiac pacemaker electrodes. *Med. & Biol. Eng.*, **6**, 579.

KAHN, A. and GREATBATCH, W. (1974) Physiological electrodes. In *Medical engineering*, RAY, C. D. (Ed.) Year Book Med. Publ.

MCDONALD, J. R. (1971) Electrical response of materials containing space charge with discharge at the electrodes. *J. Chem. Phys.*, **54**, 2026.

MOHILNER, D. M., KREUSER, J. C., NAKADOMARI, H. and MOHILNER, P. R. (1976) Computer controlled differential capacitance measurements. *J. Electrochem. Soc.*, **123**, 359.

MURDOCK, C. C. and ZIMMERMAN, E. E. (1936) Polarization impedance at low frequencies. *Physics*, **7**, 211.

RANDLES, J. E. B. (1947) Kinetics of rapid electrode reactions. *Disc. Faraday Soc.*, **1**, 11.

SCHEIDER, W. (1977) Real-time measurement of dielectric relaxation of biomolecules: kinetics of a protein-ligand binding reaction. *Ann. N. Y. Acad. Sci.*, **303**, 47.

SCHWAN, H. P. (1963) Determination of biological impedances. In *Physical techniques in biological research* (Vol. 6). NASTUK, W. L. (Ed.) Academic Press, New York, 323–407.

SCHWAN, H. P. and MACZUK, J. G. (1965) Electrode polarization impedance: limits of linearity. *Proc. 18th Ann. Conf. Eng. Biol. Med.*, **5**, 24.

SCHWAN, H. P. (1966) Alternating current electrode polarisation. *Biophysik*, **3**, 181.

SCHWAN, H. P. (1968) Electrode polarisation impedance and measurements in biological materials. *Ann. N. Y. Acad. Sci.*, **148**, 191.

SILVERMAN, H. T., MILLER, I. F. and SALKIND, A. J. (1973) *Electrochemical bioscience and bioengineering.* Electrochemical Soc., Inc., p. 160, discussion of the paper by PIERSMA *et al.*

SIMPSON, R. W. (1976) *Nonlinear electrode polarization impedance.* Ph.D. Dissertation, Univ. Pennsylvania.

SIMPSON, R. W., BERBERIAN, J. G. and SCHWAN, H. P. (1980) Nonlinear AC and DC Polarization of Platinum Electrodes. IEEE T rans., **BME-27,** 166–171.

SLUYTERS-REHBACH, M. and SLUYTERS, J. H. (1970) Sine wave methods in the study of electrode processes. *J. Electroanal. Chem*, **4,** 1.

TIMMER, B., SLUYTERS-REHBACH, M. and SLUYTERS, J. H. (1968) On the impedance of galvanic cells. XXIII. Electrode Reactions with Specific Adsorption of the Electroactive Species: the $Pb^{+2}/Pb(Hg)$ Electrode in M KNO_3-KCl Mixtures. *J. Electroanal. Chem.*, **18,** 93.

VENKATESH, S. D. and CHIN, T. (1979) The alternating current electrode processes. *Israel J. Chem.*, **18,** 56.

WARBURG, E. (1899) Ueber das Verhalten sogenannter unpolarisirbarer Elektroden gegen Wechselstrom. *Ann. Physik und Chemie*, **67,** 493.

WARBURG, E. (1901) Ueber die Polarisations capacität des Platins. *Ann. der Physik*, **6,** 125.